

# SIMULATION ANALYSIS AND TEST OF EDEM-BASED TWIN SPIRAL PROPELLER FOR MUDFLAT AQUACULTURE

## 基于 EDEM 的滩涂养殖双螺旋推进器仿真分析与试验

Maomao ZOU<sup>1)</sup>; Rui ZHANG<sup>\*1)</sup>, Xiwen ZHANG<sup>1)</sup>, Xiaoning HE<sup>1)</sup>, Shuqi SHANG<sup>13)</sup>, Xuegeng CHEN<sup>12)</sup>, Zhenjia MA<sup>1)</sup>, Moxian LI<sup>1)</sup>, Yunkang LI<sup>1)</sup>, Wenjie LI<sup>1)</sup>, Haozhe WEI<sup>1)</sup>, Yutao LI<sup>1)</sup>

<sup>1)</sup> College of Mechanical and Electrical Engineering, Qingdao Agricultural University, Qingdao 266109, China;

<sup>2)</sup> Shihezi University, Shihezi, 832003, China;

<sup>3)</sup> Key Laboratory of Intelligent Agricultural Machinery and Equipment for Saline and Alkaline Land, Ministry of Agriculture and Rural Development, 266109, China;

Tel: +86-15963011651; E-mail: 15963011651@163.com

Corresponding author: Rui ZHANG

DOI: <https://doi.org/10.35633/inmateh-72-66>

**Keywords:** mudflat aquaculture; amphibious device; discrete element simulation; twin spiral propeller; EDEM

### ABSTRACT

Aiming at the problems of coastal ecological damage and low yield of mudflat aquaculture caused by the invasion of *M. alterniflora*, in order to improve the operational efficiency of mudflat wet and soft ground, and to promote the ecological balance and the development of coastal agriculture, a walking device with twin spiral propellers for muddy wet and soft ground was designed. Using EDEM simulation software to simulate and analyze, the discrete element model of muddy soil particles is established to analyze the interaction mechanism with the spiral propeller and the operation propulsion effect, and it is concluded that the spiral propeller will not produce congestion phenomenon during the operation; data are collected through several simulation tests, and the optimal parameter design of the spiral propeller structure is derived from the response surface analysis, and the spiral propeller is designed to operate at a speed of 2.416 mph in the simulation with the optimal parameter of structural design. The field test shows that the optimal height of the spiral blades is 50 mm, the total length of the drum is 2,970 mm, the helix angle of lift is 30°, the pitch is 453 mm, and the propelling speed is 2.36 m/s. The data collected through several simulation tests are used to find the optimal parameter design of the spiral propeller structure, and the simulation speed of the spiral propeller in the optimal structural design parameter is 2.416 m/s.

### 摘要

针对互花米草入侵导致沿海生态破坏, 滩涂养殖业低产等问题, 为了提高滩涂湿软地面作业效率, 促进生态平衡与沿海农业发展, 设计一种泥泞湿软地面双螺旋推进器行走装置。利用 EDEM 仿真软件进行仿真分析, 建立泥泞土壤颗粒的离散元模型, 分析其与螺旋推进器的互作机理与作业推进效果, 并探究得出螺旋推进器在作业时不会产生壅土现象; 通过多次仿真试验搜集数据, 经响应面分析得出螺旋推进器结构的最佳参数设计, 螺旋推进器在最佳结构设计参数的仿真推进速度为 2.416m/s。田间试验验证表明, 在滚筒直径为 400 mm, 螺旋叶片最佳高度为 50 mm; 滚筒总长为 2 970 mm, 螺旋升角为 30°, 螺距为 453mm, 作业推进速度为 2.36m/s。

### INTRODUCTION

Mudflats are special landforms at the junction of ocean and land, which make them a unique ecosystem due to factors such as their geographic location and climatic environment. The invasion of *M. alterniflora*, which is native to the United States (Shang et al., 2009), will compete for nutrients with the aquaculture products in the mudflat, leading to a substantial reduction in the production of shellfish, algae, fish and crabs, etc. In addition, *M. alterniflora* also affects the exchange capacity of seawater, which leads to a decline in water quality and induces red tides, and the large-scale flooding of *M. alterniflora* may also affect the smoothness of the waterway and impede the traffic of the harbors and terminals. As shown in Figure 1, effective management and control of the breeding and expansion of exotic species of *M. alterniflora* is urgent (Qiao et al., 2019; Gao, 2021).

Maomao ZOU, Ph.D. Stud. Eng.; Rui ZHANG\*, Prof. Ph.D. Eng.; Xiwen ZHANG, Ph.D. Stud. Eng.; Xiaoning HE, Prof. Ph.D. Eng.; Shuqi SHANG, Prof. Ph.D. Eng.; Xuegeng CHEN, Prof. Ph.D. Eng.; Zhenjia MA, Ph.D. Stud. Eng.; Moxian LI, Ph.D. Stud. Eng.; Yunkang LI, Ph.D. Stud. Eng.; Wenjie LI, Ph.D. Stud. Eng.; Haozhe WEI, Ph.D. Stud. Eng.; Yutao LI, Ph.D. Stud. Eng.



Fig. 1 - Coastal mudflats invaded by *M. alterniflora*

The current measures to control and remove *M. alterniflora* (Ji et al., 2023; Zhou et al., 2023; Yin et al., 2023) mainly include physical, chemical and biological techniques, however, the above techniques still have the problems of poor management effect, secondary pollution to the environment, and even ecological damage. Mechanical physical cleanup, as an environmentally friendly removal method, has received close attention from the industry. However, the offshore mudflat ground is always in a wet and muddy state, which makes it extremely inconvenient for the walking and transportation of conventional equipment (Wei, 2019). In the face of muddy and wet mudflat ground represented by mudflats, ordinary land walking equipment often produces skidding and falling into the situation, which results in the difficulty of the operation of the conventional land walking equipment, and the development of the corresponding means of transportation due to the special geography has always been a difficult problem. In order to improve the transportation efficiency and throughput rate of such terrain, scholars at home and abroad have done a lot of research and developed many different types of walking devices, which mainly include: ordinary wheeled, tracked, multi-wheeled wide-wheeled, spiral propulsion, air cushion carrier and so on. Through checking the references, it is concluded (Guo et al., 2014) that among these five main types of muddy ground transportation, the air cushion transportation type has the lowest value of ground specific pressure, and the higher the value of ground specific pressure, the higher the pressure on the ground, and the easier it is to sink in the muddy ground; conversely, the less likely it is to sink in the muddy ground, and the higher the efficiency of walking. Air cushion transportation and handling is the use of gas film technology to lift and move the load, it is widely used in the field of aviation, precision or heavy instrument handling, such as airships to the launcher, transportation costs are high, not suitable for application in the field of agricultural machinery operations.

In the case of the spiral propulsion vehicle, because the ground pressure is small, the driving force is large, so the performance is strong. It is especially suitable for driving in some extreme soft and muddy terrain road surface. Spiral propulsion vehicle uses the spiral propeller as a walking mechanism; the spiral propeller is generally installed on both sides of the walking device as its main walking mechanism, through the spiral propeller and ground media (water, soil, etc.) to achieve the mutual action of the device to move forward, through the reverse rotation of the spiral propeller to achieve the device moving backward, through the two sides of the spiral propeller differential rotation to achieve the device steering walk. In the fluid, semi-fluid ground, the hollow structure of the spiral propeller can play the role of float, can effectively reduce the pressure value, so that the vehicle is not easy to fall into the ground.

The pressure value of the spiral propulsion transportation mode is second only to that of air cushion transportation, and it is a kind of idealized transportation tool suitable for traveling and operating on wet, soft and muddy ground such as river and sea shoals and marshes through the comprehensive consideration of feasibility, versatility and economy.

In order to promote the protection of offshore mudflat ecosystems and the development of coastal mudflat aquaculture and agriculture, as well as to reduce the cost and improve the efficiency of invasive species management, a shallow mudflat traveling device based on a twin-spiral propeller was designed.

## MATERIALS AND METHODS

### *General structure and working principle*

#### ● General structure of the traveling device

The traveling device is mainly composed of diesel engine, twin spiral propeller, wide crawler chassis, hydraulic lifting system, reduction gearbox, class hull and other parts, as shown in Fig. 2.

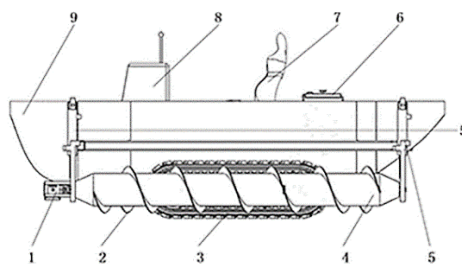


**Fig. 2 - Twin spiral propeller walking device structure diagram**

1. Gearbox; 2. Spiral blade; 3. Crawler walking device; 4. Spiral roller; 5. Hydraulic lifting device; 6. Diesel engine; 7. Driver's seat; 8. Operation desk; 9. Class hull

● **Working principle of twin spiral propeller walking device**

The walking device adopts diesel engine as the power source, the power of diesel engine is transmitted to the crawler gearbox through the belt to drive the crawler to walk, and then the power is transmitted to the two sides of the spiral propeller through the gear reducer box, universal drive shaft, coupling and other components to drive the spiral propeller blade to interact with the water or silt, and the reaction force is utilized to drive the walking device to realize the operation of the device.

In the offshore beach operation, this device can walk with the wide track, when encountering the phenomenon of slipping and sinking of the track on the wet and muddy ground, and the tracked walking device cannot work normally or the operation efficiency is low; it can be operated by the hydraulic lifting device through the hydraulic control handle to move down the two sides of the spiral propeller (the rotating bearing seat of the spiral propeller is connected with the hydraulic rod), so that the propeller is in contact with the ground media and the main driving wheel of the track is supported, and the propeller blades interact with the water or silt. The main driving wheel of the crawler will transfer the power to the spiral propeller through the gearbox and transmission shaft, and the rotation of the spiral propeller will realize the traveling through the mutual action with the medium.

When the tide of offshore beach operation is high, this device can float in the offshore by virtue of the hull, at this time the two sides of the spiral propeller can be used as a propeller to provide the device with power in the water, to realize the water travel.

**Kinematic analysis of a twin spiral propeller**

● **Preliminary design of the parameters of the twin-screw propeller**

By reviewing the relevant literature and learning to refer to other similar structure of the screw propulsion of the operating machine tools (*Sheludchenko Bogdan et al., 2022; Opeyemi Oladunjoye, 2022*), and then after the preliminary data collection and research on the key structural parameters of the screw propeller drum diameter, helical angle of lift, helical blade height, and blade pitch parameter combination analysis (*Feng et al., 2020*), the preliminary design of the structural parameters of the screw propeller reference range of values is shown in Table 1.

**Table 1**

Preliminary parameterization for screw propellers		
Title	Parameters	Unit
Blade Height/d	30~70	mm
Drum diameter/D	375~425	mm
Pitch of blade/J	425~500	mm
Helix angle of lift/ $\alpha$	25~35	°

**Discrete Element Modelling and Simulation Analysis**

In order to determine the forward direction of the spiral propeller will not produce congestion phenomenon in the actual work and to determine the walking propulsion speed under different combinations of structural parameters of the spiral propeller, EDEM discrete element simulation software is used to establish a simulation model of the spiral propeller-muddy soil particles, simulate the interactions between the machine tools and the soil in the actual work, and collect multiple sets of parameters for response surface analysis to explore the optimal parameter combinations of the spiral propeller, which will provide a basis for the subsequent field experiments and optimization of the structure.

● **Discrete elemental modelling of soil particles**

Muddy soil particle model is the key factor affecting the simulation test results, according to the related research, combined with soil particle size test and related research, according to the soil characteristics of offshore beach mudland, query its soil property parameters, the soil particles were approximated to be set as a spherical model, and the radius was set to 3 mm, as shown in Fig. 3 (Fang et al., 2016; Zeng et al., 2023).

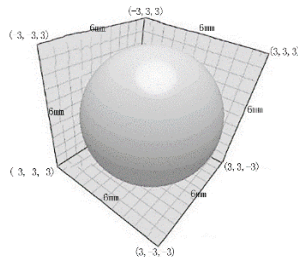


Fig. 3 - Discrete element model of soil particles

● **Modeling of soil tanks and spiral propellers**

A semi-cylindrical soil trough with a radius of 250 mm and a length of 4,510 mm was drawn using SolidWorks 3D design software and a particle factory was set up in it to generate and release soil particles, the material of the soil trough was pine wood with a density of 340 kg/m<sup>3</sup>; the model of the spiral propeller was imported and fixed in the soil trough, the material of the spiral propeller was 316 stainless steel with a density of 8,000 kg/m<sup>3</sup>, as shown in Figure 4. The combined 3D model of soil tank and spiral propeller was saved in STL format and imported into EDEM software.

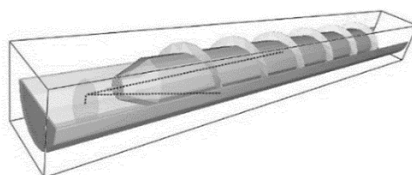


Fig. 4 - Modelling of soil flume and spiral propeller

● **Contact parameter**

The density of offshore beach soil is 1 700 kg/m<sup>3</sup>, Poisson's ratio is 0.5, modulus of elasticity is 3.5×10<sup>6</sup> N/m<sup>2</sup>, soil cohesion is 5 to 10 kPa, and the kinetic friction factor between the spiral propeller and the soil is 0.45 to 0.6, and the static friction factor is 0.76 (Liu et al., 2015; Guo, 2016; Chen, 2023). The specific contact parameter ranges were determined based on relevant studies as well as the slant test method, as shown in Table 2.

Table 2

EDEM simulation contact parameter table		
Title	Parameters	Unit
Soil intensity	1700	kg/m <sup>3</sup>
Poisson's ratio for soil	0.5	/
Soil cohesion	5~10	kPa
Spiral propeller – soil (kinetic friction factor)	0.45~0.6	/
Spiral propeller – soil (static friction factor)	0.76	/
Soil modulus of elasticity	3.5×10 <sup>6</sup>	N/m <sup>2</sup>

**RESULTS**

● **Simulation tests**

In order to simulate the actual working condition of the spiral propeller, a soil tank model was established with a radius of 250 mm and a length of 4,510 mm, which can make the generated soil particles completely wrap the spiral propeller, and in order to make the experiments closer to the real operating conditions, three particle factories were set up in the soil tank, which were located in front of the spiral propeller, in front of the left side, and at the back of the right side, respectively, to generate 80,000, 25,000, and 20,000 soil particles, the particle generation speed was 1.5 m/s, and the simulation was started.

Figures 5 to 8 show the simulation test of the interactions with soil particles during the operation of the spiral propeller and the velocity change of the soil particles (Zhao et al., 2023; Song et al., 2021; Hong, 2019).

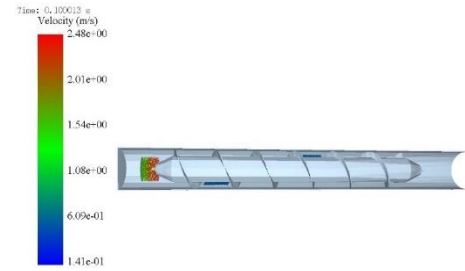


Fig. 5 - 0.1s simulation test process

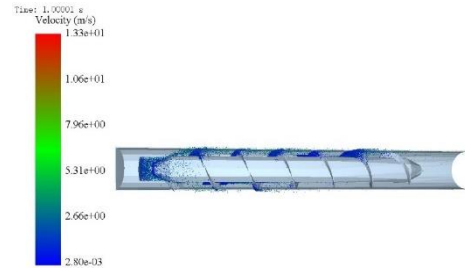


Fig. 6 - 1s simulation test process

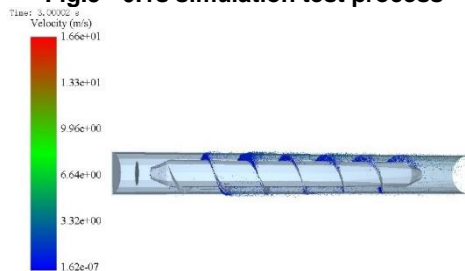


Fig. 7 - 3s simulation test process

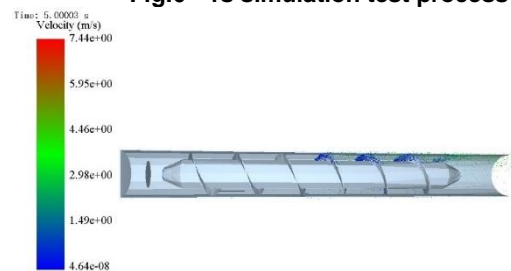


Fig. 8 - 5s simulation test process

During the experimental process, as the particle plant generates particles, the spiral propeller rotates at a speed of 4 rad/s for the soil displacement test, and the test processes of 0.1 s, 1 s, 3 s, and 5 s were recorded, respectively, and the experimental results show that the spiral propeller discharges the soil with good effect and does not generate the phenomenon of soil congestion.

In order to investigate the optimal structural parameters of the spiral propeller, several combinations of spiral propeller structural parameters (as shown in Table 3) were designed to simulate the propulsion speed and collect data.

Table 3

Experimental coding table				
Level	Experimental factors			
	Drum diameter / mm	Helix angle of lift / °	Spiral blade height / mm	Pitch of blade / mm
-1	375	25	30	425
0	400	30	45	462.5
1	425	35	70	500

The propulsive velocity data of the spiral propeller under different combinations of structural parameters were obtained through multifactor and multilevel simulation tests, as shown in Table 4:

Table 4

Response surface test results					
Number of tests	Experimental factors				
	Drum diameter / mm	Helix angle of lift / °	Spiral blade height / mm	Pitch of blade / mm	Speed of advancement / (m/s)
1	400	25	50	425	2.192
2	400	25	70	462.5	2.01
3	375	25	50	462.5	2.17
4	425	30	70	462.5	2.071
5	375	30	30	462.5	2.03
6	400	30	30	425	2.07
7	425	35	50	462.5	2.145
8	425	30	50	500	2.16

Number of tests	Experimental factors				
	Drum diameter / mm	Helix angle of lift / °	Spiral blade height / mm	Pitch of blade / mm	Speed of advancement / (m/s)
9	400	35	30	462.5	2.03
10	425	30	50	425	2.13
11	400	35	50	425	2.12
12	400	30	70	425	2.022
13	400	35	70	462.5	1.97
14	375	30	50	425	2.16
15	375	30	70	462.5	2.05
16	425	25	50	462.5	2.197
17	400	30	50	462.5	2.49
18	400	35	50	500	2.2
19	400	30	50	462.5	2.431
20	400	25	30	462.5	2.07
21	400	30	50	462.5	2.456
22	375	30	50	500	2.12
23	425	30	30	462.5	2.186
24	375	35	50	462.5	2.23
25	400	25	50	500	2.19
26	400	30	30	500	2.1
27	400	30	70	500	2

Table 5

Regression model ANOVA						
Source of variance	Square sum	Degrees of freedom	Mean square	F-value	P-value	Significance
<b>Model</b>	0.4 362	14	0.0 312	17.23	<0.0 001	<b>Significant</b>
<b>A Drum diameter</b>	0.0 014	1	0.0 014	0.7 667	0.3 984	
<b>B Helix angle of lift</b>	0.0 015	1	0.0 015	0.8 273	0.3 810	
<b>C Spiral blade height</b>	0.0 110	1	0.0 110	6.07	0.0 298	
<b>D Pitch of blade</b>	0.0 005	1	0.0 005	0.2 661	0.6 153	
<b>AB</b>	0.0 031	1	0.0 031	1.73	0.2 125	
<b>AC</b>	0.0 046	1	0.0 046	2.52	0.1 385	
<b>AD</b>	0.0 012	1	0.0 012	0.6 773	0.4 266	
<b>BC</b>	0.0 000	1	0.0 000	0.0 000	1.0 000	
<b>BD</b>	0.0 017	1	0.0 017	0.9 294	0.3 540	
<b>CD</b>	0.0 007	1	0.0 007	0.3 738	0.5 524	
<b>A2</b>	0.0 939	1	0.0 939	51.90	<0.0 001	
<b>B2</b>	0.1 173	1	0.1 173	64.85	<0.0 001	
<b>C2</b>	0.3 680	1	0.3 680	203.45	<0.0 001	
<b>D2</b>	0.1 294	1	0.1 294	71.57	<0.0 001	

Source of variance	Square sum	Degrees of freedom	Mean square	F-value	P-value	Significance
Residual	0.0 217	12	0.0 018			
Lost item	0.0 199	10	0.0 020	2.27	0.3 438	Insufficient
Pure error	0.0 018	2	0.0 009			
Sum of all	0.4 579	26				
R <sup>2</sup>	0.9 526					
R <sup>2</sup> A <sub>adj</sub>	0.8 973					

The quadratic polynomial regression equation obtained from the analysis of variance (ANOVA) of the results of the spiral propeller propulsive velocity sensory scoring test using the Design-Expert 13 software is:

$$\begin{aligned}
 Y = & 2.46 + 0.0108A - 0.0112B - 0.0302C + 0.0063D \\
 & - 0.0280AB - 0.0337AC + 0.0175AD + 0.0000BC \\
 & + 0.0205BD - 0.0130CD - 0.1327A^2 - 0.1483B^2 \\
 & - 0.2627C^2 - 0.1558D^2
 \end{aligned}
 \tag{1}$$

The regression model ANOVA results are shown in Table 5.

The interaction between AC (drum diameter and helical blade height) was the most significant (P = 0.1 385) as shown in Figure 9 by ANOVA in Table 5. The optimum combination of structural parameters is shown in Table 6.

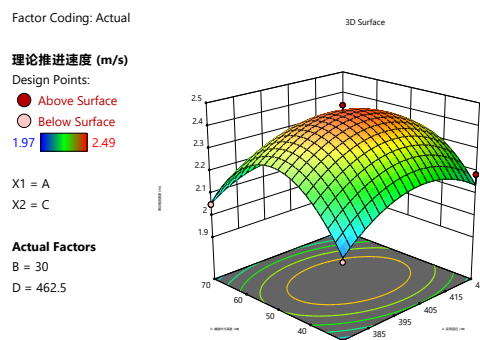


Fig. 9 - Response surface variation chart

Table 6

Optimal parameter combinations for spiral propellers		
Title	Parameters	Unit
Blade Height / d	48.7 687	mm
Drum diameter / D	401.35	mm
Pitch of blade / J	463.363	mm
Helix angle of lift / α	29.7 953	°
Maximum propulsion speed / v	2.49	m/s

**Test Equipment and Methods**

● **Field trials**

In order to further examine the discharge propulsion capability of the designed twin spiral propeller in practical work, combined with the theoretical calculation analysis and simulation test results, a field test was conducted on April 18, 2023, in the coastal mudflat of the Blue Seed Industry Park in Wendeng District, Weihai City, Shandong Province, as shown in Figure 10.

The operating parameters of the spiral propeller selected for the test were: the diameter of the drum was 400 mm, the height of the spiral blade was 50 mm; the total length of the drum was 2,970 mm, the helical lift angle was 30°, and the pitch was 453 mm; and the traveling speed was 2.36 m/s at a diesel engine speed of 3,200 rpm.



Fig.10 - Field test of twin-spiral propeller traveling device

Relationships between slip rate, sinkage and screw propeller speed were analyzed separately in field tests. The data was also collected and plotted on a line graph using Origin software, as shown in Figures 11 and 12:

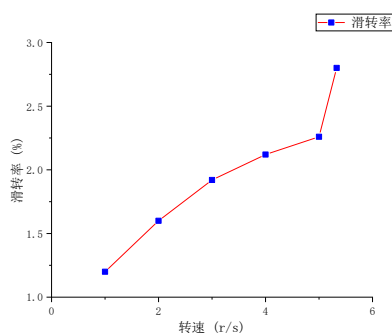


Fig. 11 - Rotation speed-slip rate relationship

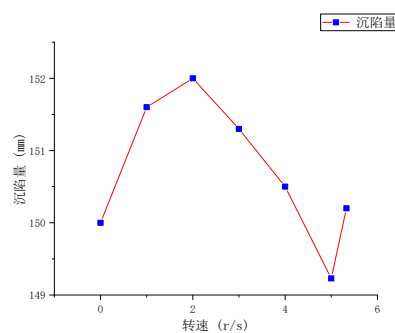


Fig. 12 - Rotation speed-sinkage relationship

## CONCLUSIONS

(1) Through the study of the physical characteristics of muddy soil in coastal beaches, a spiral propeller travel device suitable for walking on muddy land was designed, and the key parameters of the spiral propeller were analyzed to obtain the optimal parameter combination of the structure.

(2) The discrete element method was used to establish a model of muddy soil particles in mud flats, and simulation analysis was carried out with the height of the spiral propeller blades and the helix angle of the blades as the test factors, and with the propelling speed of the walking device and whether congestion occurs in front of the device as the test indexes, and finally it was concluded that the designed spiral propeller does not produce congestion.

(3) The field test shows that the test results are basically consistent with the simulation results, under the design of 400 mm drum diameter, 50 mm helical blade height, 2,970 mm drum length, 30° helical angle of lift and 453 mm pitch, the propeller does not generate congestion in the forward direction, and the propulsion speed of the device reaches 2.36 m/s. The design is also consistent with the simulation results, and the design is consistent with the simulation results, and the propulsion speed of the device reaches 2.36 m/s.

## ACKNOWLEDGEMENT

This research received financial support from the Key R&D Program of Shandong Province, China (No.2022CXGC010401). Thanks to the International Field Test Mechanization Association for providing us with the research foundation and platform.

## REFERENCES

- [1] Chen Z.X. (2023). Research on the effect of grouting lifting to reinforce soil body and preventing well wall rupture [D] (注浆抬升加固土体及防治井壁破裂效果研究). *China University of Mining and Technology*, 001042.
- [2] Fang H.M, Ji C Y. (2016). Analysis of soil motion behavior during rotary tillage based on discrete element method [J] (基于离散元法的旋耕过程土壤运动行为分析). *Journal of Agricultural Machinery*, 47(3):22-28.
- [3] Feng G., Zhou Y., Tu M. (2020). Design and test of spiral-propelled lotus root digger [J] (螺旋推进式挖

- 藕机的设计与试验) . *Journal of Gansu Agricultural University*, 55(04):191-199.
- [4] Gao R. (2021). Impacts of mutualistic ricegrass invasion on soil physicochemical properties of coastal wetland in Huangjiatangwan [D] (互花米草入侵对黄家塘湾滨海湿地土壤理化性质的影响) . *Qufu Normal University*, 000744.
- [5] Guo T.T. (2016). Experimental study on the effect of consolidation ratio on kinetic properties of pulverized clay [J] (固结比对粉质粘土动力学特性影响的试验研究) . *Advances in Geophysics*, 31(06): 2729-2734.
- [6] Guo X.L, Liu J., Zhao Y. (2014). Overview of the current research status of spiral-propelled vehicles [J] (螺旋推进车研究现状概述) *Agricultural Equipment and Vehicle Engineering*, 52(04):14-17+27.
- [7] Hong D.W. (2019). Research on the friction mechanical characteristics of oil pine root system and soil in the loess area of west Jin [D] (晋西黄土区油松根系与土壤的摩擦力学特性研究) . *Beijing Forestry University*, 001123.
- [8] Ji Y. L., Pu S.C., Song Y. (2023). Impacts of *M. alterniflora* invasion on macrobenthos of salt marsh wetland in Yushan Bay [J] (互花米草入侵对乳山湾盐沼湿地大型底栖动物的影响) . *Journal of Aquatic Sciences*, 36(05):77-84.
- [9] Liu Y., Chang X.Y., Li H.N. (2015). Relationships between salinity, conductivity and water content of grassy beach soils in typical coastal beaches in northern Jiangsu Province [J] (苏北典型滨海滩涂草滩土壤盐度、电导率与含水率的关系) . *Water Saving Irrigation*, (08):4-7.
- [10] Opeyemi Oladunjoye, Christina Maffattone (2022). Omnidirectional All-Terrain Spiral-Driven Robot Design, *Modeling and Application in Humanitarian Demining*, 55(27):7-12.
- [11] Qiao P.Y, Wang A.D., Xie B.H. (2019). Effects of herbicides on the invasive plant *Miscanthus intermedium* in the Yellow River Delta [J] (除草剂对黄河三角洲入侵植物互花米草的影响) . *Journal of Ecology*, 39(15):5627-5634.
- [12] Qiao P.Y. (2019). Research on physical and chemical control of invasive plant *Miscanthus intermedium* in the Yellow River Delta [D] (黄河三角洲入侵植物互花米草物理、化学防治研究). *Inner Mongolia University*.
- [13] Shang X., Guan W.B., Zhang G.S. (2009). Impacts of *M. alterniflora* invasion on the food web of estuarine salt marsh wetlands [J] (互花米草入侵对河口盐沼湿地食物网的影响). *Journal of Oceanography*, 31(01):132-142.
- [14] Sheludchenko Bogdan, Šarauskis Egidijus, Kukharets Savelii, Zabrodskiyi Andrii. (2022). Graphic analytical optimization of design and operating parameters of tires for drive wheels of agricultural machinery [J]. *Soil & Tillage Research*, 215,105227.
- [15] Song S.L, Tang Z.H., Zheng X. (2021). Calibration of discrete element parameters of a post-tillage soil model for cotton fields in Xinjiang [J] (新疆棉田耕后土壤模型离散元参数标定) . *Journal of Agricultural Engineering*, 37(20):63-70.
- [16] Wei X.W. (2019). Design and simulation research of automatic harvesting equipment for beach mutualistic rice grass [D] (滩涂互花米草自动收割设备设计及仿真研究) . *Dalian Ocean University*, 000134.
- [17] Yin X.L, Tan C.Y., Ke Y.H. (2023). Patterns of landscape pattern evolution and driving factors of coastal salt marsh wetlands in the Yellow River Delta from 1973 to 2020 [J/OL] (1973—2020年黄河三角洲滨海盐沼湿地景观格局演化模式和驱动因素) . *Journal of Ecology*, 2024, (01):1-14.
- [18] Zeng M.J, Cong J.L., Yan Q. (2023). Design and test of chopping anti-clogging system of forage rape harvester [J/OL] (饲用油菜收获机切碎防堵系统的设计与试验) . *Journal of Shihezi University (Natural Science Edition)*, 1-9.
- [19] Zhao Z., Wang D.W., He X.N., Shang S.Q., Zheng X.S., Zhu H., Xia C., Shi Y.X. (2023). Analysis and test of EDEM-based rotary tillage device for oil salsa bean [J] (基于 EDEM 的油莎豆旋耕装置分析与试验) . *Agricultural Mechanization Research*, 45(05):173-179.
- Zhou Y., Jiang Z.J., Qiu G.L. (2023). Distribution of seagrass resources in China, causes of degradation and protection measures [J] (中国海草资源分布现状、退化原因与保护对策) . *Ocean and Lake*, 54(05):1248-1257.